

Research on the Identification Algorithm of Crayfish Body Features Based on the Improved Yolov8n Loss Function

Md Shahazul Islam^{1*}, Md Musa Haque², Md Salman³, Md Shahin Ali⁴, Shaykat Purokayisto⁵

¹ Information and Communication Engineering, Nanjing University of Information Science and Technology, Nanjing, China

² International American University, Los Angeles, California, USA

^{3,4,5} Artificial Intelligence, Nanjing University of Information Science and Technology, Nanjing, China

* Correspondence Email: shahazul5410@gmail.com | 202352180013@nuist.edu.cn

doi: <https://doi.org/10.37745/ijeats.13/vol12n41734>

Published November 09, 2024

Citation: Islam M.S., Haque M.M., Salman M., Ali M.S., and Purokayisto S. (2024) Research on the Identification Algorithm of Crayfish Body Features Based on the Improved Yolov8n Loss Function, *International Journal of Engineering and Advanced Technology Studies*, 12 (4), 17-34

Abstract: *The crayfish industry, primarily focused on *Procambarus clarkii*, is expanding rapidly but encounters challenges due to inadequate automation. Traditional manual visual inspection methods used for evaluating crayfish size and integrity during breeding and processing are labor-intensive and prone to errors. This study presents an improved algorithm based on the YOLOv8n framework to intelligently recognize and grade crayfish by accurately detecting the body, tail, and claws of *Procambarus clarkii*. The proposed approach introduces innovation by replacing the original loss function CIoU (Complete Intersection over Union) with MPDIoU (Modified Perfect Dark Intersection over Union). A novel scale factor, denoted as the ratio, has been introduced to adjust the size of the auxiliary bounding box within the loss calculation framework. This improvement, in conjunction with the MPDIoU loss function, notably enhances the accuracy and efficiency of bounding box regression. As a result, it enables the precise detection of the distinct body parts of crayfish, a pivotal advancement in automating the grading process. Empirical assessments demonstrated substantial enhancements in recognition accuracy. The incorporation of Inner-MPDIoU into the YOLOv8n model elevated the mean Average Precision (mAP) from 83.7% to 90.8% across IoU thresholds ranging from 0.5 to 0.95. The results of this study highlight the effectiveness of the proposed algorithm in precisely recognizing critical elements of *Procambarus clarkii*. This investigation contributes to the overarching goal of attaining intelligent and accurate grading within the crayfish domain, potentially transforming conventional practices and enhancing industry productivity. The implications transcend mere automation, providing a groundwork for future exploration into intelligent systems tailored to the unique requirements of the crayfish industry.*

Keywords: *Procambarus clarkii*; image recognition; YOLOv8; MPDIoU; deep learning

INTRODUCTION

In recent years, the scale and output value of *Procambarus clarkii* aquaculture have reached new highs, with a cultivation area of 18670000 hm², The output was 2.8907 million tons, an increase of 7.69% year-on-year and 9.6%[1]. Different markets have different requirements for the specifications of *Procambarus clarkii*[2]. Currently, the sorting of specifications for commercial *Procambarus clarkii* is mainly done manually, relying on the accumulated experience of workers to judge the integrity, vitality, and specifications of *Procambarus clarkii* before dividing them. The process involves subjectivity and variability among individual workers, resulting in significant errors in the division results. Additionally, the manual division process takes a long time, leading to a decrease in the vitality of *Procambarus clarkii* and a high stress mortality rate, resulting in significant economic losses.

With the continuous development of deep learning, object detection provides technical support for precision farming, fish behavior monitoring, quantity statistics, and identification of aquatic product diseases in the aquaculture industry. Utilized transfer learning and inter layer fusion mechanisms to identify 10 fish species with complex background[3]. The experimental results show that the model can improve the classification and recognition ability of fish in complex underwater scenes, and provide support for the study of fishery resource distribution. In deep learning models, the YOLO (You Only Look Once) series belongs to end-to-end networks and is widely used due to its fast detection speed[4]. Zhang et al.[5] used attention mechanism, feature fusion, and K-means++ clustering algorithm to improve the detection accuracy of YOLOv5 for small target bacteria, solving the problems of low efficiency and large errors in manual counting of fish pathogenic bacteria. Li et al.[6] replaced the original Bottleneck with Res2Net residual structure and coordinate attention mechanism based on YOLOv5, achieving accurate and fast fish detection methods in fisheries. Wang et al.[7] used the DP-YOLO model and combined it with the dynamic detection gate algorithm to avoid duplicate counting of tuna. The proposed method for evaluating miscounting error indicators achieved an automatic counting accuracy of 97% for catch 9% provides a new idea for automatic statistics of catch in offshore fisheries. YOLOv8 is the latest algorithm in the YOLO series, which has improved detection accuracy compared to other algorithms in the series[8]. Li et al.[9] proposed the YOLOv8 Head ECAM method for detecting fish populations in aquaculture, which increases the size of the detection head in FPN to better capture the detailed information of underwater fish individuals. The ECAM attention mechanism is used to reduce the interference of blurry backgrounds, which can better adapt to situations where underwater fish populations are blurry or obstructed. Huangfu et al.[10] improved the backbone network GCBLOCK structure based on the YOLOv8 model to address the problems of high labor costs and heavy workload in traditional commercial fishing vessel monitoring fish detection and recognition tasks. They increased feature extraction capabilities and used a new convolution method called GSConv to reduce model computation. They replaced the loss

function CIoU with SIoU to achieve fish detection and recognition in commercial fishing vessel electronic monitoring data at a lower cost.

Compared with other aquaculture organisms, the development of large-scale aquaculture of *Procambarus clarkii* was relatively late, and there is little research on its intelligence. Combining the application of deep learning to other organisms, it is introduced into the *Procambarus clarkii* industry to recognize the body, claws, and tail of commercial *Procambarus clarkii*, and promote the intelligent development of related industries of *Procambarus clarkii*. When annotating various parts of the *Procambarus clarkii*, it was found that the border overlap was high, which affected the accuracy of the detection results. To minimize this impact, a method was proposed to combine Inner IoU with MPDIoU instead of the original CIoU to improve the accuracy and efficiency of bounding box regression, achieving better detection accuracy to a certain extent.

MATERIALS AND METHODS

Experimental environment configuration and data preparation

Environment deployment

The overall flowchart of this study is shown in Figure 1. Using the YOLOv8n model cloned from the official website and utilizing it on the PyCharm platform GPU for training, GPU model NVIDIA GTX3060, CUDA version 12.1 Python version 3.11 The CPU is R5-5600 and the operating system is Windows 11 Professional Edition.

Data preparation

This study takes the *Procambarus clarkii* as the experimental object. In order to facilitate the application of the research results in practical industrial scenarios, the dataset images used are all with a single white background to enhance the consistency of image processing and the generalization ability of the model. The dataset images were captured in a laboratory environment using an Android phone's built-in camera. *Procambarus clarkii* purchases different specifications of commercial shrimp for the market. Due to the limited sample size, image enhancement processing was performed on the data to expand the dataset, improve the adequacy of model training, and enhance the model's generalization ability. The specific methods include various enhancement operations such as mirror flipping (Figure 2b), grayscale processing (Figure 2c), and adding noise (Figure 2d) to the original image (Figure 2a).

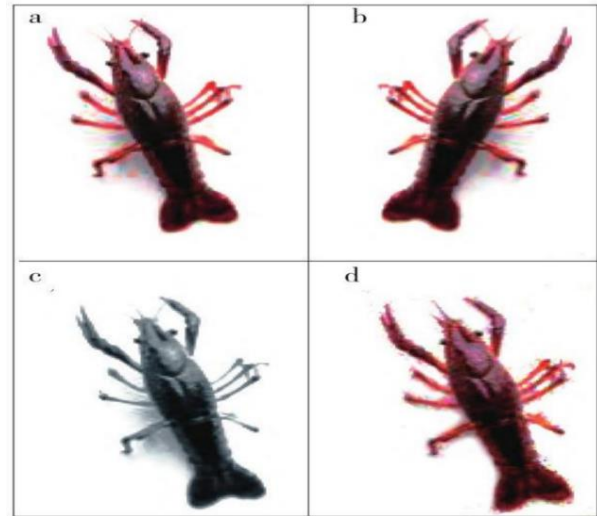
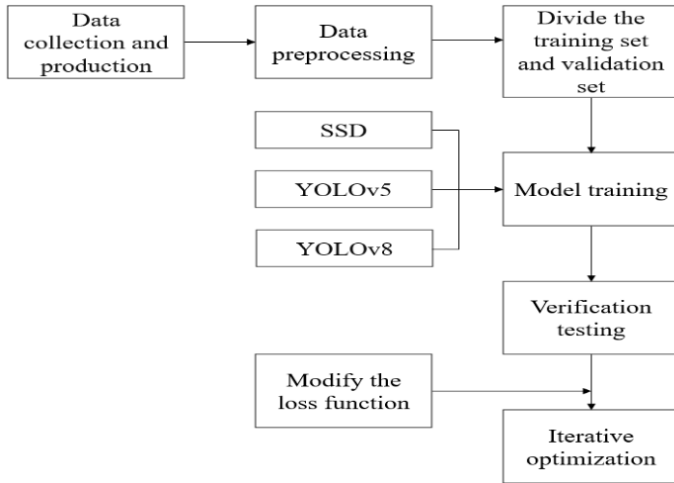


Fig. 1 Flowchart for the identification of crayfish

Fig. 2 Dataset image augmentation

The Labeling annotation tool[11] was used to accurately label the images of *Procambarus clarkii*, which were mainly divided into three parts: Crayfish, Aofoot, and Tail. Each part was individually labeled and saved as a text file (txt format) according to the requirements of YOLO data format. The annotation process is shown in Figure 3.

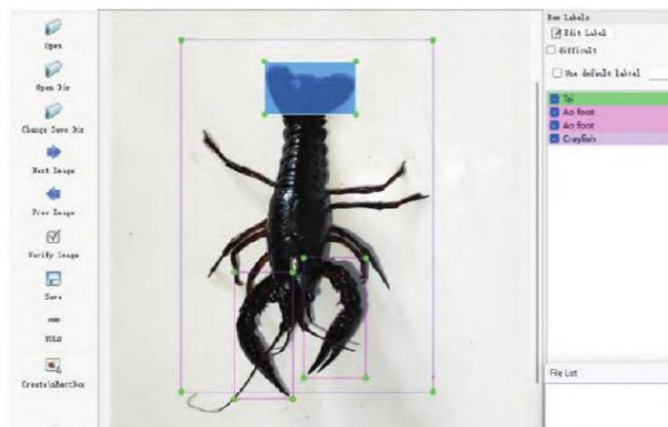


Fig. 3 Dataset annotation

Divide the processed dataset of 1073 images into a training set and a validation set in a 9:1 ratio, and place them together with the generated label files into the YOLOv8 project for training. Set the number of experimental iterations to 200.

Identification method of *Procambarus clarkii* based on improved YOLOv8n improvement of YOLOv8n

YOLOv8 provides a new SOTA model that combines the advantages of YOLO series functions and makes some improvements[12]. It includes five models, namely YOLOv8n, YOLOv8s, YOLOv8m, YOLOv8l, and YOLOv8x. Among them, YOLOv8n is the lightest model, mainly divided into four parts: Input, Backbone, Neck, and Head[13]. This study will be improved based on YOLOv8n.

The loss function is a function that calculates the difference between the predicted value (P) and the true value (G), and the smaller the loss value, the more successful the model is[14]. Calculate as shown in formula (1):

$$L_{IoU} = \frac{P \cap G}{P \cup G} \quad (1)$$

Inner IoU calculates the IoU loss through auxiliary bounding boxes and introduces a scale factor to control the scale size of the auxiliary bounding boxes for different datasets and detectors to compensate for the lack of generality in IoU based bounding box regression loss [15]. Inner IoU defines formulas (2) to (8) as follows:

$$b_l^g = x_c^g - \frac{w^g \cdot r}{2}, b_r^g = x_c^g + \frac{w^g \cdot r}{2} \quad (2)$$

$$b_t^g = y_c^g - \frac{h^g \cdot r}{2}, b_b^g = y_c^g + \frac{h^g \cdot r}{2} \quad (3)$$

$$b_l = x_c - \frac{w \cdot r}{2}, b_r = x_c + \frac{w \cdot r}{2} \quad (4)$$

$$b_t = y_c - \frac{h \cdot r}{2}, b_b = y_c + \frac{h \cdot r}{2} \quad (5)$$

$$i = [\min(b_r^g, b_r) - \max(b_t^g, b_t)] \cdot [\min(b_b^g, b_b) - \max(b_t^g, b_t)] \quad (5)$$

$$b_b) - \max(b_t^g, b_t)] \quad (6)$$

$$u = (w^g \cdot h^g) \cdot r^2 + (w \cdot h) \cdot r^2 - i \quad (7)$$

$$L_{IoU}^I = \frac{i}{u} \quad (8)$$

In the formula: g represents Ground Truth; (x_c^g, y_c^g) represents the center point between the real bounding box and the interior of the real bounding box; (x_c, y_c) represents the center point of the anchor frame and the inner needle frame; x 、 y 、 w 、 h represent the center coordinates, width, and height of the bounding box, respectively; r represents the scale factor ratio, typically ranging from [0.5, 1.5]; l (Localization) represents localization loss; c (Confidence) represents the accuracy of the model's prediction of object categories; t (Threshold) represents the threshold of the ratio factor; i represents the inter intersection, which refers to the area where the predicted bounding box b overlaps with the real bounding box b^g ; u represents the total area of the predicted bounding box and the real bounding box, including their intersection and non overlapping areas; I (inner) represents using an auxiliary inner box to calculate IoU loss; IoU stands for Intersection over Union, which is the ratio of the overlap area between the predicted bounding box and the true bounding box to their union.

Inner IoU retains the characteristics of IoU, with a value range of [0,1]. Compared with IoU loss, when the ratio is <1 and the size of the auxiliary bounding box is smaller than the actual bounding box, the effective range of regression is smaller than the IoU loss, but the absolute value of the gradient is greater than the gradient obtained by IoU loss, which can accelerate the convergence of high IoU samples. On the contrary, when the ratio is greater than 1, larger auxiliary bounding boxes expand the effective range of regression and enhance the effectiveness of regression for low IoU samples.

YOLOv8 adopts the Task Aligned Assign positive sample allocation strategy and introduces Distribution Focal Loss in loss calculation. The category loss uses cross entropy loss, and the bounding box regression uses DFL Loss+CIoU Loss [16]. The bounding box regression loss mainly considers three important geometric factors: overlap area, central point distance, and aspect ratio [17]. CIoU [18] includes these three factors, and the calculation formulas (9) to (11) are as follows:

$$L_{\text{CIoU}} = L_{\text{IoU}} - \frac{\rho(b_g, b_p)}{c^2} - \alpha V \quad (9)$$

$$V = \frac{4}{\pi^2} \left(\arctan \frac{w^g}{h^g} - \arctan \frac{w^p}{h^p} \right)^2 \quad (10)$$

$$\alpha = \frac{V}{1 - L_{\text{IoU}} + V} \quad (11)$$

In the formula, ρ represents the Euclidean distance between the center points of two bounding boxes; p represents the predicted bounding box; c is a scale factor used to adjust the influence of the distance term from the center point; V represents aspect ratio consistency, which is used to measure the difference in

aspect ratio between predicted bounding boxes and real bounding boxes; α is a positive balancing parameter used to balance the impact of aspect ratio consistency term V .

When the predicted bounding box and the real bounding box have the same aspect ratio but different width and height values, most existing loss functions will lose their effectiveness, limiting convergence speed and accuracy. The MPDIoU loss function simplifies the similarity comparison between the predicted bounding box and the true bounding box by minimizing the distance between the upper left and lower right points, and can adapt to overlapping or non overlapping bounding box regression[19]. The MPDIoU calculation formula (12) is as follows:

$$L_{\text{MPDIoU}} = L_{\text{IoU}} - \frac{d_1^2}{w^2 + h^2} - \frac{d_2^2}{w^2 + h^2} \quad (12)$$

In the formula, d_1, d_2 are the squared Euclidean distances from the upper left corner of the predicted bounding box to the upper left and lower right corners of the actual bounding box, respectively; w, h represents the actual width and height of the bounding box.

Evaluation Indicators

The accuracy and precision of model training are generally determined by mAP (mean Average Precision) values [20][21][22]. MAP 0.5 refers to the mAP value at the 50% IoU threshold; Calculate mAP 0 at 0.5, it will be at 0.5 to 0 Within the IoU range of 0.95, with 0 To evaluate the performance of the model, the average mAP value under different IoU thresholds is taken to obtain a comprehensive evaluation index, referred to as mAP. Precision refers to the proportion of correct samples among all predicted samples; Recall reflects the proportion of correctly classified samples in the total sample. This research model will use Precision, Recall, and mAP as evaluation metrics for the experiment [23].

RESULTS AND DISCUSSION

Ablation Test

To verify the effectiveness of Inner MPDIoU in improving the YOLOv8n algorithm, multiple experiments were conducted on the dataset and ablation experiments were designed. Precision (P), recall (R), and mAP were selected as performance evaluation metrics [24]. The ablation experiment [25] is based on the original YOLOv8n algorithm and sequentially introduces Inner IoU and MPDIoU. The results of the ablation experiment are shown in Table 1.

Table 1. Ablation experiment

Model	Accuracy (P)	Recall (R)	Average Accuracy (mAP)
YOLOv8n	98.1%	97.5%	83.7%
YOLOv8n+Inner-IoU	98.9%	99.5%	89.5%
YOLOv8n+Inner-MPDIoU	99.3%	99.7%	90.8%

According to Table 1, after introducing the Inner IoU algorithm into the YOLOv8n model, its already high accuracy and recall were further enhanced by 0.7% and 2%. In addition, the average precision (mAP) has significantly improved by 5.8%. This indicates that the Inner IoU algorithm has a significant positive impact on improving model performance.

When introducing the MPDIoU loss function into the model, its performance was further optimized. Compared with the original model, the improved model achieved performance in the three key indicators of P, R and mAP 1.2%, 2.2% and 7.1% growth. This result fully confirms the effectiveness of the Inner MPDIoU module and the strategy of introducing a ratio factor to control the size of auxiliary bounding boxes, which can significantly improve the accuracy of bounding box regression and the overall efficiency of the model.

In summary, the introduction of the Inner MPDIoU module, combined with the assistance of the ratio factor, not only enhances the model's ability to handle bounding box regression tasks, but also improves the model's recognition accuracy for the research object. This improvement is crucial for object detection tasks, especially in complex scenes that require high-precision recognition. This method can better meet the needs of research and application.

Model Comparison Experiment

The classic algorithms for object detection include YOLO, SSD algorithm, etc. [26], and YOLOv5 is one of the classic algorithms in the YOLO series[27]. To verify the effectiveness of Inner MPDIoU in identifying various parts of *Procambarus clarkii*, a comparative experiment was conducted between YOLOv8n, SSD, and YOLOv5s algorithm models. The dataset images and labels used by each model were completely consistent, that is, the XML label files used by SSD were converted from the TXT label file format used by YOLOv5 and YOLOv8.

4. The training and recognition results of the SSD model on *Procambarus clarkii* are shown in Figure 4.

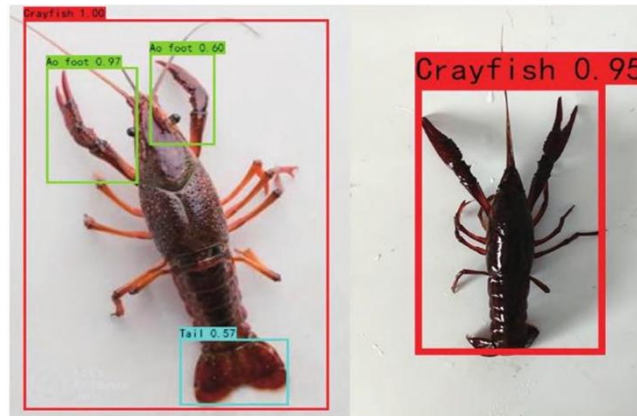


Fig. 4 SSD detection effect diagram

As shown in Figure 4, the SSD model performs well in identifying the body of *Procambarus clarkii*, with an extremely high level of accuracy. However, the performance of the SSD model in identifying claws and shrimp tails is not satisfactory. Specifically, the model has low accuracy in identifying claws and shrimp tails, and there is a certain degree of missed detection, which may have adverse effects on accurate evaluation and automated processing.

From Figure 5, it is found that the average accuracy of the SSD model in identifying the tail of *Procambarus clarkii* is only 47%, which is much lower than the recognition accuracy of the shrimp body in the model. In addition, the overall average accuracy of the model is 76%. Although this indicator may be sufficient in some application scenarios, for situations that require higher recognition accuracy, such as fine aquatic processing or high-precision aquaculture monitoring, the current model performance clearly needs to be improved.

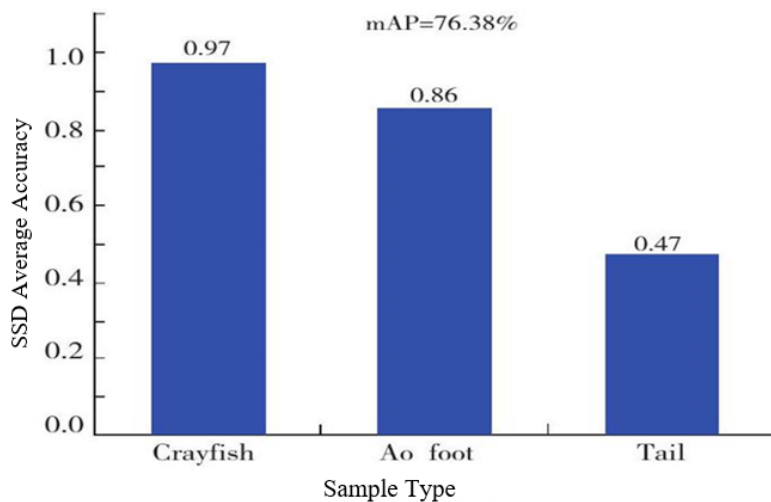


Fig. 5 SSD Average Precision

In addition to the issue of recognition accuracy, the training process of SSD models is also time-consuming. According to the training results of the model, the training time of the model reached 4612 hours. In application scenarios that require rapid iteration and immediate feedback, this training time may become a bottleneck that limits the application of the model. Although the SSD model performs well in certain recognition tasks, further optimization and improvement are still needed in the recognition of the claws and tails of *Procambarus clarkii*.

The overall recognition performance has reached a high level, indicating that the model has strong applicability and effectiveness in handling such object detection tasks. However, for individuals with damaged tails of *Procambarus clarkii*, the recognition accuracy of the YOLOv5s model significantly decreased. This indicates that the model has a high dependence on the integrity of the tail of *Procambarus clarkii*, and any damage or incompleteness may have a negative impact on the recognition results. Therefore, for individuals with tail damage, additional algorithm optimization or data augmentation strategies may be needed to improve the robustness of the model.

The training and recognition results of YOLOv5s model on *Procambarus clarkii* are shown in Figure 6.



Fig. 6 YOLOv5s detection effect diagram

In addition, the total training time of YOLOv5s model is 5564 h, compared to other evaluation models, it takes the longest time. The current training rate may not meet the high efficiency requirements of applications such as online aquatic monitoring or automated sorting systems.

The training results of the improved YOLOv8 model in this study are shown in Figure 7.

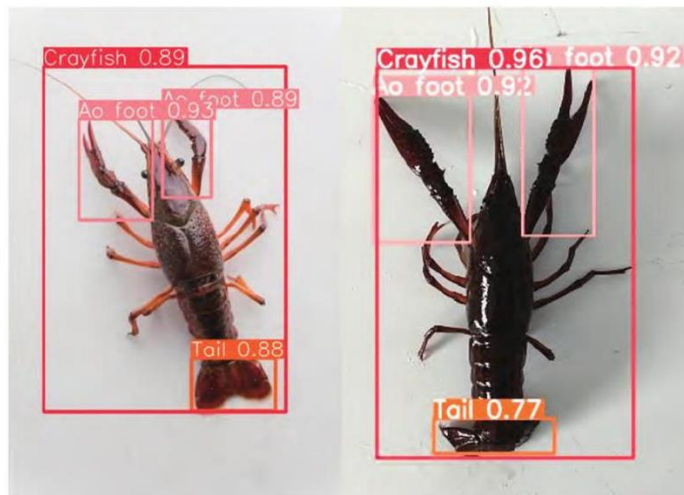


Fig. 7 YOLOv8_Inner_MPDlou detection effect diagram

Compared with the YOLOv5s model, the improved YOLOv8 model showed similar high-level performance in recognition accuracy. However, the model used in this study performed better in terms of the balance of recognition accuracy for various parts. That is, even in the case of incomplete tail of the target object, the improved YOLOv8 model still had higher recognition accuracy than the YOLOv5s model, and its training process was significantly accelerated, taking only 2043 hours is less than 50% of the training time of the YOLOv5s model. This significant time reduction makes YOLOv8 more advantageous in real-time detection scenarios, as it can adapt to dynamically changing environments more quickly and effectively meet the needs of fast iteration and instant feedback.

Figure 8 shows the mAP value curves of the three models mentioned above. Both YOLO models have a recognition accuracy close to 1 compared to the SSD model, which is superior to the SSD model. The difference in recognition accuracy between YOLOv5s and the improved YOLOv8 model is relatively small, while the latter has a faster learning speed and relatively better training performance.

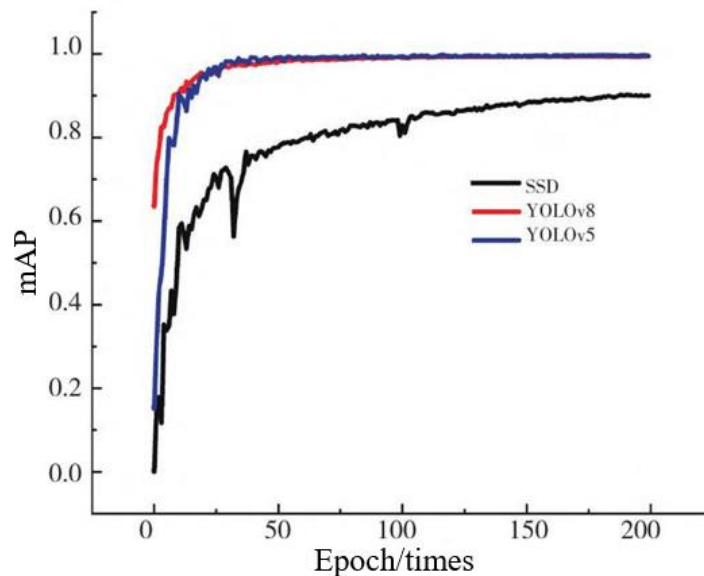


Fig. 8 Different models value of mAP

Figure 9 shows the mAP curves of YOLOv5s and the improved YOLOv8 model. The improved YOLOv8 model has slightly higher accuracy within the mAP range than YOLOv5s. This small but consistent improvement in accuracy has resulted in higher reliability and lower false alarm rates in the actual detection process of body features in *Procambarus clarkii*.

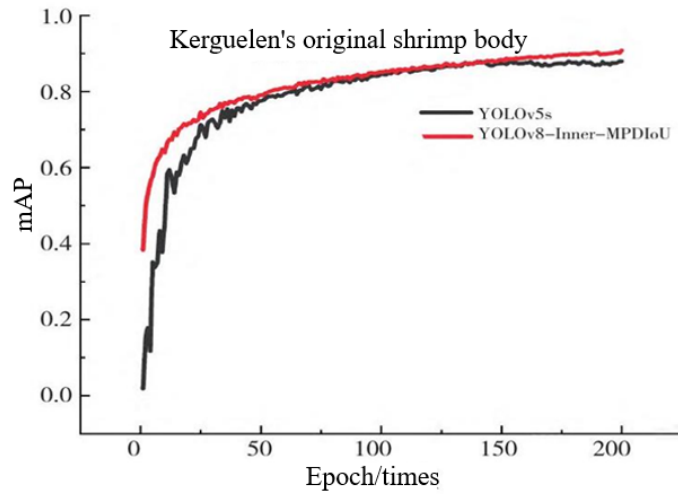


Fig. 9 mAP of YOLOv5s and improved YOLOv8

Inner MPDIoU recognition results

To verify the performance of Inner MPDIoU in recognizing various parts of *Procambarus clarkii*, the recognition results and normalized confusion matrix are shown in Table 2 and Figure 10.

Table 2. Inner-MPDIoU crayfish parts Identification results

Part names of <i>Procambarus clarkii</i>	P	R	mAP
Crayfish	99.3%	100%	97.0%
Aofoot	99.6%	99.6%	91.9%
Tail	99.0%	99.5%	83.5%

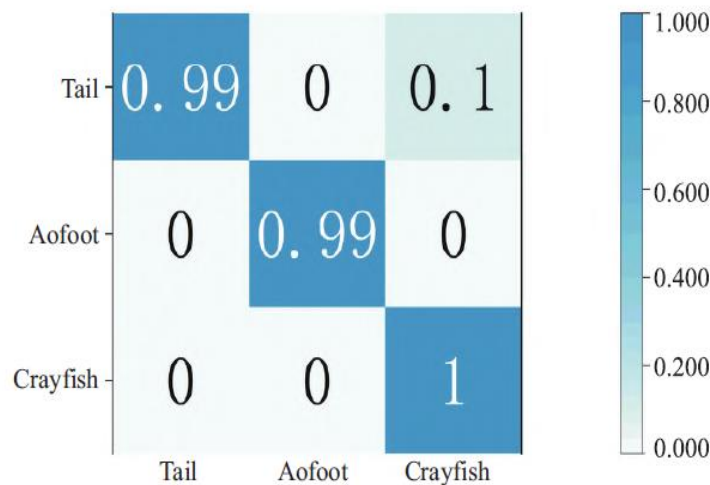


Fig. 10 Crayfish parts identification results normalized confusion matrix

According to Table 2, the accuracy and recall rates of various parts of the *Procambarus clarkii* have reached over 99%, especially the recall rate of "Aofoot" has reached 1; Crayfish "occupies the largest area and is easy to identify, with an mAP of 97% and the best recognition effect; The "Grayfish" feature is obvious, and the mAP has also reached 91.9%; Tail "is influenced by the movement or posture of the *Procambarus clarkii*, with its tail often curled up and obscured by its body, resulting in poor recognition performance. The mAP only reached 83.5%, the overall accuracy of the model reached 90.8%. According to the normalized confusion matrix in Figure 10, the diagonal from the top left corner to the bottom right corner represents the recognition accuracy of each classification, and the area outside the diagonal represents the misclassified area [28]. The classification accuracy of each part reaches 99%, proving the good stability of the model.

The training loss curve of the model intuitively reflects the learning dynamics of the model during training, which is an important basis for determining whether the model converges and whether there are overfitting problems. As shown in Figure 11, the training loss curve of the improved YOLOv8 model shows that there is a small difference between the training loss and the validation loss, indicating that the model has good training performance and good generalization ability. The smooth downward trend of the loss curve further confirms the stability of the model training process.

In the field of object detection, different types of aquatic animals pose varying degrees of challenges to recognition tasks due to their unique physiological structures and behavioral habits. Compared to the recognition of South American white shrimp[29][30], the recognition task of *Procambarus clarkii* in this

study faces more complex challenges. The claw foot volume of *Procambarus clarkii* is relatively large, which leads to an increase in the overlap between pre selected boxes in the image, thereby increasing the difficulty of bounding box regression. Overlapping bounding boxes not only make it difficult for the model to distinguish, but may also cause a significant decrease in the regression rate and accuracy of the bounding boxes, which poses a challenge to the recognition performance of the model.

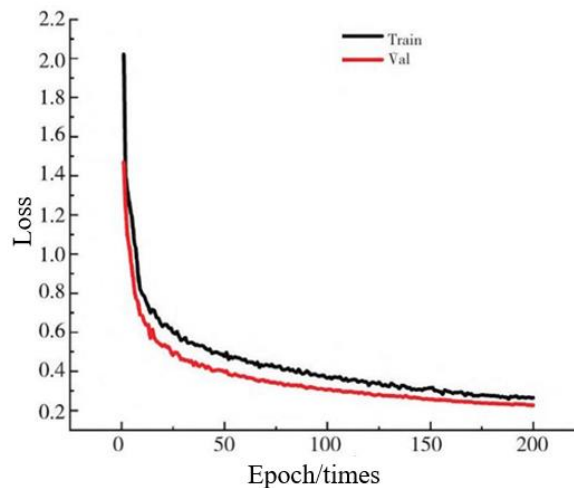


Fig. 11 Crayfish parts loss

In response to this issue, this study introduces the Inner IoU loss function, which significantly improves the calculation accuracy of the bounding box scale size. By using the Inner IoU loss function, the model can more accurately calculate the scale of the auxiliary bounding box, thereby effectively guiding the regression of the bounding box in the loss calculation. In addition, the MPDIoU loss function was also used in the study, which was specifically designed to reduce the problem of decreased recognition performance caused by border overlap. Through these improvements, the YOLOv8 model demonstrated even better performance in the recognition task of *Procambarus clarkii*. The model not only improves the accuracy of bounding box regression, but also maintains high recognition accuracy when facing complex situations with overlapping borders. The integration of these technologies significantly enhances the recognition effect of YOLOv8 on *Procambarus clarkii*, providing strong technical support for automation and intelligence in aquaculture, biological monitoring, and other related fields.

CONCLUSION

This study proposes an improved YOLOv8n model that replaces the traditional CIoU loss function with the Inner MPDIoU loss function, significantly reducing the problem of decreased recognition accuracy caused by bounding box overlap in target detection for *Procambarus clarkii*, and effectively improving the

recognition accuracy of the model. The research results provide new technical support for the intelligent recognition technology of *Procambarus clarkii*, which is of great significance for promoting the intelligent and automated upgrading of the industry. Through precise target detection, the efficiency and accuracy of crayfish farming, classification, and even disease monitoring can be greatly improved. However, this experiment was conducted in a controlled laboratory environment and may not fully simulate the complex behavior of *Procambarus clarkii* in natural environments. Given the high activity and diverse postures of *Procambarus clarkii* in natural environments, this dynamic characteristic may result in only capturing some of their features in practical application scenarios under fixed angle and single camera position shooting conditions. This limitation increases the difficulty of comprehensive identification of *Procambarus clarkii*. Therefore, future research needs to further explore more advanced algorithms and strategies to better adapt to the recognition needs of the dynamic characteristics of *Procambarus clarkii*. This may include but is not limited to data collection from multiple angles and positions, time series analysis, and further optimization of deep learning models. Through these efforts, more accurate and comprehensive identification of *Procambarus clarkii* can be achieved in the future.

REFERENCES

- [1] Wang, J., Wang, Z., Wang, Q. and Zhou, Z., 2023. Ecological index analysis of growth and development of *Procambarus Clarkii* based on biological characteristics. *Journal of Sea Research*, 192, p.102363.
- [2] Wang, J., Wang, Z., Wang, Q. and Zhou, Z., 2023. Ecological index analysis of growth and development of *Procambarus Clarkii* based on biological characteristics. *Journal of Sea Research*, 192, p.102363.
- [3] Jiang, L., Quan, H., Xie, T. and Qian, J., 2022. Fish recognition in complex underwater scenes based on targeted sample transfer learning. *Multimedia Tools and Applications*, 81(18), pp.25303-25317.
- [4] Pham, M.T., Courtrai, L., Friguet, C., Lefèvre, S. and Baussard, A., 2020. YOLO-Fine: One-stage detector of small objects under various backgrounds in remote sensing images. *Remote Sensing*, 12(15), p.2501.
- [5] Zhang, Y., Duan, H., Liu, Y., Li, Y. and Lin, J., 2023. Converge of coordinate attention boosted YOLOv5 model and quantum dot labeled fluorescent biosensing for rapid detection of the poultry disease. *Computers and Electronics in Agriculture*, 206, p.107702.
- [6] Li, L., Shi, G. and Jiang, T., 2023. Fish detection method based on improved YOLOv5. *Aquaculture International*, 31(5), pp.2513-2530.
- [7] Wang, C., Wang, Q., Qian, Y., Hu, Y., Xue, Y. and Wang, H., 2023. DP-YOLO: Effective Improvement Based on YOLO Detector. *Applied Sciences*, 13(21), p.11676.
- [8] Safaldin, M., Zaghden, N. and Mejdoub, M., 2024. An Improved YOLOv8 to Detect Moving Objects. *IEEE Access*.

- [9] Li, Z., Luo, S., Xiang, J., Chen, Y. and Luo, Q., 2024. Improved Chinese Giant Salamander Parental Care Behavior Detection Based on YOLOv8. *Animals*, 14(14), p.2089.
- [10] Huangfu, Z., Li, S. and Yan, L., 2024. Ghost-YOLO v8: An Attention-Guided Enhanced Small Target Detection Algorithm for Floating Litter on Water Surfaces. *Computers, Materials & Continua*, 80(3).
- [11] Jiang, H., Xing, Z., Lu, W., Qian, Z., Yu, H. and Li, J., 2014. Transcriptome analysis of red swamp crawfish *Procambarus clarkii* reveals genes involved in gonadal development. *PloS one*, 9(8), p.e105122.
- [12] Jia, C., Wang, D., Liu, J. and Deng, W., 2024. Performance Optimization and Application Research of YOLOv8 Model in Object Detection. *Academic Journal of Science and Technology*, 10(1), pp.325-329.
- [13] Jinbo, G., Shenghuai, W., Xiaohui, C., Chen, W. and Wei, Z., 2024. QL-YOLOv8s: Precisely optimized lightweight YOLOv8 pavement disease detection model. *IEEE Access*.
- [14] Zhao, H., Gallo, O., Frosio, I. and Kautz, J., 2016. Loss functions for image restoration with neural networks. *IEEE Transactions on computational imaging*, 3(1), pp.47-57.
- [15] Sun, Y., Wang, J., Wang, H., Zhang, S., You, Y., Yu, Z. and Peng, Y., 2024. Fused-IoU Loss: Efficient Learning for Accurate Bounding Box Regression. *IEEE Access*.
- [16] Zheng, Z., Wang, P., Liu, W., Li, J., Ye, R. and Ren, D., 2020, April. Distance-IoU loss: Faster and better learning for bounding box regression. In *Proceedings of the AAAI conference on artificial intelligence* (Vol. 34, No. 07, pp. 12993-13000).
- [17] Zheng, Z., Wang, P., Ren, D., Liu, W., Ye, R., Hu, Q. and Zuo, W., 2021. Enhancing geometric factors in model learning and inference for object detection and instance segmentation. *IEEE transactions on cybernetics*, 52(8), pp.8574-8586.
- [18] Xue, J., Cheng, F., Li, Y., Song, Y. and Mao, T., 2022. Detection of farmland obstacles based on an improved YOLOv5s algorithm by using CIoU and anchor box scale clustering. *Sensors*, 22(5), p.1790.
- [19] Ma, S. and Xu, Y., 2023. MpdIoU: a loss for efficient and accurate bounding box regression. *arXiv preprint arXiv:2307.07662*.
- [20] Mao, R., Zhang, Y., Wang, Z., Hao, X., Zhu, T., Gao, S. and Hu, X., 2024. DAE-Mask: a novel deep-learning-based automatic detection model for in-field wheat diseases. *Precision Agriculture*, 25(2), pp.785-810.
- [21] Micikevicius, P., Narang, S., Alben, J., Diamos, G., Elsen, E., Garcia, D., Ginsburg, B., Houston, M., Kuchaiev, O., Venkatesh, G. and Wu, H., 2017. Mixed precision training. *arXiv preprint arXiv:1710.03740*.
- [22] Girshick, R., Donahue, J., Darrell, T. and Malik, J., 2015. Region-based convolutional networks for accurate object detection and segmentation. *IEEE transactions on pattern analysis and machine intelligence*, 38(1), pp.142-158.

- [23] Bylinskii, Z., Judd, T., Oliva, A., Torralba, A. and Durand, F., 2018. What do different evaluation metrics tell us about saliency models?. *IEEE transactions on pattern analysis and machine intelligence*, 41(3), pp.740-757.
- [24] Padilla, R., Netto, S.L. and Da Silva, E.A., 2020, July. A survey on performance metrics for object-detection algorithms. In *2020 international conference on systems, signals and image processing (IWSSIP)* (pp. 237-242). IEEE.
- [25] Wang, J., Liu, M., Du, Y., Zhao, M., Jia, H., Guo, Z., Su, Y., Lu, D. and Liu, Y., 2024. PG-YOLO: An efficient detection algorithm for pomegranate before fruit thinning. *Engineering Applications of Artificial Intelligence*, 134, p.108700.
- [26] Adarsh, P., Rathi, P. and Kumar, M., 2020, March. YOLO v3-Tiny: Object Detection and Recognition using one stage improved model. In *2020 6th international conference on advanced computing and communication systems (ICACCS)* (pp. 687-694). IEEE.
- [27] Ting, L., Baijun, Z., Yongsheng, Z. and Shun, Y., 2021, July. Ship detection algorithm based on improved YOLO V5. In *2021 6th International Conference on Automation, Control and Robotics Engineering (CACRE)* (pp. 483-487). IEEE.
- [28] Steele, B.M., Winne, J.C. and Redmond, R.L., 1998. Estimation and mapping of misclassification probabilities for thematic land cover maps. *Remote sensing of environment*, 66(2), pp.192-202.
- [29] Setiawan, A., Hadiyanto, H. and Widodo, C.E., 2023. Internet of Things for Underwater Shrimp Image Detection Using Blob Detector. *International Journal on Advanced Science, Engineering & Information Technology*, 13(3).
- [30] Zhou, H., Kim, S.H., Kim, S.C., Kim, C.W., Kang, S.W. and Kim, H., 2023. Instance segmentation of shrimp based on contrastive learning. *Applied Sciences*, 13(12), p.6979.